Materials Science Forum
ISSN: 1662-9752, Vol. 1188, pp 95-105

Submitted: 2026-02-02
Revised: 2026-02-17
Accepted: 2026-02-22
Online: 2026-04-20

Cleaner Melt Transfer of Recycled Aluminium Alloys: Simulation-Guided Launder Baffle Design for Aerospace-Grade Structural Castings

Tharmalingam Sivarupan[1,a*], Arul Mozhi Varman Jayaraman Palanivel[1,b], Konstantinos Georgarakis[1,c], John Forde[2,d], Ben Shaw[3,e], Konstantinos Salonitis[1,f], Mark Jolly[1,g]

[1]Sustainable Manufacturing Systems Centre, Faculty of Engineering and Applied Sciences, Cranfield University, United Kingdom,

[2]JF Advanced Technology Solutions Ltd., Warwickshire, United Kingdom,

[3]Sylatech Ltd., York, United Kingdom

Corresponding Author: [a]siva.sivarupan@cranfield.ac.uk, [b]a.jayaramanpalanivel@cranfield.ac.uk, [c]k.georgarakis@cranfield.ac.uk, [d]john.forde@jfatechsolutions.com, [e]benshaw@sylatech.com, [f]k.salonitis@cranfield.ac.uk, [g]m.r.jolly@cranfield.ac.uk

Keywords: Aluminium alloys, impurity elements, baffle, sedimentation, simulation, sustainability, aerospace castings, HPC.

Abstract. Cleaner melt transfer is critical to the broader use of recycled aluminium alloys in high-end structural casting applications, where oxide bifilms and intermetallic inclusions, such as Fe-containing intermetallics, can significantly affect the casting's mechanical properties. In counter-gravity low- and high-pressure casting, the launder system must not only promote the sedimentation of inclusions but also deliver a stable, cleaner melt to the crucible. Prior research showed that 15° double baffles in the mid-section of the sedimentation launder at a flow rate of 100 $kg \cdot h^{-1}$ provide high efficiency. The present work investigates the influence of baffle design at the launder-crucible interface, where the melt enters the crucible before casting. Fluid dynamic simulations were carried out at a 100 $kg \cdot h^{-1}$ flow rate for three inlet configurations: (i) full baffle; (ii) lifted baffle; and (iii) split baffle. Inclusions of various densities and diameters were tracked. Results indicate that the full baffle, while beneficial as a benchmark and efficient, is impractical because it generates fresh oxide surfaces. The lifted baffle provided the most effective reduction in inclusions, like the full baffle setup, enhancing sedimentation and suppressing entrainment, while the split baffle showed intermediate behaviour. Moreover, the lifted configuration promoted centrifugal flow (at lower velocities, it still made a partial contribution) within the crucible, directing inclusions towards the crucible wall and the stagnation-velocity zone, and enabling the crucible itself to act as a final sedimentation stage before the counter-gravity pump extracts the melt. These results demonstrate that combining mid-launder optimisation with crucible inlet baffle design enables cleaner, more automated melt delivery, thereby strengthening the use of recycled aluminium alloys in structural casting applications.

Introduction

The adoption of secondary (recycled) aluminium alloys for structural and high-integrity cast components, such as those utilised in aerospace applications, is an environmentally friendlier option. A key barrier is melt cleanness; oxide bifilms, often referred to as double-oxide “bifilms”, and intermetallic inclusions introduced during melting and transfer can severely reduce fatigue life and increase tolerance levels in mechanical properties. Secondary contamination occurs when melt-flow disruptions expose fresh metal surfaces to air, leading to the formation of an oxide bifilm and re-entrainment. This underscores the importance of maintaining stable flow and designing baffles appropriately for the casting melt delivery system. Campbell’s bifilm framework links entrained surface oxides to crack-like internal defects that govern fracture and fatigue performance of the casting[1]. Quantification approaches, such as the ‘bifilm index’ proposed by Dispinar and Campbell, have provided practical melt-quality metrics that correlate with mechanical properties [2].

Experimental studies of bifilm behaviour in Al-Si-Mg alloys further confirm that bifilms form during turbulent handling and are the dominant defect-controlling factor [3]. Therefore, delivering a cleaner melt to the mould cavity for structural casting is a prime choice.

Flow-conditioning devices, such as baffles, dams, and weirs, in hydraulic systems are widely used in metallurgical and civil engineering applications to tailor the residence time distribution (RTD), suppress turbulence, and create low- or stagnation-velocity zones favourable for inclusion filtration. Although a substantial portion of this literature arises from tundish metallurgy (steelmaking), the governing fluid mechanics of particle transport, RTD control, and turbulence suppression provide transferable design principles. For example, Zhang et al. demonstrated that flow control devices can significantly alter the tundish flow structure and inclusion-filtration performance [4]. More recent numerical optimisation studies show that combinations of baffles and turbulence inhibitors can increase residence time and improve inclusion-filtration efficiency across a range of particle sizes [5]. He et al., report that hydrodynamic stability improves when baffles and inhibitors are arranged to reduce short-circuiting and stagnation zones [6].

Industrial melt-cleaning routes typically combine degassing, fluxing, and filtration. However, passive separation techniques based on residence time and controlled hydrodynamics are attractive for continuous melt delivery because they can reduce reliance on consumables and avoid secondary contamination [7]. Sedimentation-based launders (or ‘settling’ launders) are intended to control fluid velocity and provide prolonged residence time to promote inclusion settling (for phases denser than the melt) or flotation (for phases less dense than the melt). The effectiveness of this approach depends strongly on the local flow field, particularly near interfaces and transition zones where recirculation, jets, or surface disturbances can cause re-entrainment. In civil engineering applications [8], at room temperature, the design of baffles or exposure of the fluid to the atmosphere may have a positive effect, as nitrogen gas adsorption can help agglomerate inclusions and is used in water treatment applications; whereas in metallurgical applications, at elevated temperature, the melt surface can react with atmospheric constituents and re-entrain, e.g., metal oxides, that is a loss of metal. Therefore, the baffle design has limited options for promoting melt flow below the surface.

In counter-gravity casting processes, the launder’s role extends beyond inclusion filtration. It must deliver a stable, clean melt to the crucible, from which the alloy is continuously extracted. Flow disturbances or poor interface design at the launder-crucible boundary can re-entrain settled inclusions or generate new oxide films. Although prior studies have shown that inclined double baffles [9], within the sedimentation launder, significantly enhancing inclusion filtration, the influence of baffle geometry at the crucible inlet has received limited or no attention.

Experimental investigation of inclusion trajectories in liquid metals is often challenging, costly and environmentally unsustainable; therefore, validation methods, e.g, positron emission particle tracking (PEPT), which was developed at Birmingham University, are valuable for comparing experimental and simulation results. Griffiths et al. [10] demonstrated the use of PEPT to track entrained inclusions in shape-casting environments, thereby providing a pathway to validate inclusion-transport models. Burnard’s thesis [11] further developed PEPT-based analysis and compared particle pathways with simulations in industrially relevant launder flows that included a baffle in the melt path. Such studies reinforce the importance of reliably capturing flow features that control particle residence and sedimentation.

In parallel, controlled filling routes, such as counter-gravity casting, have been promoted to reduce turbulence and improve melt cleanness by enabling more quiescent mould filling and by avoiding/minimising the formation of new oxide surfaces. The CRIMSON (Constrained Rapid Induction Melting Single Shot Up-Casting) concept [12], for instance, has been assessed for energy and environmental benefits and emphasises controlled, computer-guided counter-gravity filling.

Counter-gravity methods can reduce oxide entrainment at the mould, but overall cleanness still depends on stable melt transfer into the crucible and effective inclusion management before pumping/pouring.

Within Ultra Clean Cast Digital Liquid Metal Manufacturing project (UltraCleanCAST DLMM), the authors' prior research [9,13] demonstrated that inclined double baffles in the mid-section of a sedimentation launder can significantly improve inclusion retention at low flow rates, identifying 15° double baffles at a melt flow rate of 100 $kg \cdot h^{-1}$ as a strong baseline configuration. However, the launder-crucible interface remains a critical region where flow disturbances may re-entrain settled inclusions or generate new oxide surfaces. This motivates the present study, which evaluates alternative baffle configurations at the launder-crucible interface, analogous to overflow-, undershot-, and slotted-weir concepts, to control crucible inlet hydrodynamics and promote final-stage sedimentation before counter-gravity extraction. This necessitates designing and assessing alternative baffle configurations at the launder-crucible interface, using high-fidelity numerical simulations (a finite-volume method) to quantify their influence on flow behaviour, inclusion transport, and sedimentation performance. The simulation is considered high-fidelity due to (not limited to) full 3D transient **finite-volume modelling**, Lagrangian tracking of inclusions with density and size variation, long physical simulation time (~22600 s), inclusion force modelling (gravity, buoyancy, centrifugal), realistic boundary conditions and flow rate, and particle counting using flux surfaces. Hence, a binary baffle setup with a double baffle at the centre of the sediment tank and the other at the launder-crucible interface has been evaluated.

Numerical Methodology

Geometry, System Description, and Simulation

The simulated system consists of a sedimentation launder connected to a crucible in a counter-gravity casting setup. The mid-section of the launder incorporates previously optimised 15° double baffles (Figure 1), while the interface region features interchangeable baffle designs (Figure 2) evaluated in this study. The alloy melt, at 650 °C, flows from left to right toward the crucible, which then pumps the melt at the same rate as the inflow, 0.028 $kg \cdot s^{-1}$ (~100 $kg \cdot h^{-1}$). At the inlet region and just before the primary baffles, two particle generators generate inclusions of various densities (3348 $kg \cdot m^{-3}$and 3990 $kg \cdot m^{-3}$) and diameters (25 µm, 50 µm, 100 µm, and 1000 µm) at a rate of 30 s^{-1} in total and in equal portions at random. The inclusions discussed here represent the density of, e.g., Ti-/Fe-containing intermetallic inclusions (predendritic Fe-intermetallics or Ti-containing intermetallics formed due to the master alloy[1] addition) with a density of around 3348 $kg \cdot m^{-3}$ and alumina (bulk, but the density of aluminium oxide bifilm should be less than this density due to its porous nature) with a density of 3990 $kg \cdot m^{-3}$. These inclusions flow with the melt and encounter the baffles at the middle of the launder, the primary baffles at 15° angle from the vertical in the anticlockwise direction, and then the vertical baffle at the launder-crucible interface, the secondary baffle, Figure 2. The baffle setup was designed to influence the flow patterns of the melt and these inclusions; hence, the inclusions could be sedimented in the middle of the launder at the sediment tank or within the crucible and not escape the system, thereby keeping the melt supplied by the system cleaner for counter-gravity casting.

Although the geometry is symmetric, a full geometry simulation was necessary, despite its computational intensity, because inclusion transport is inherently asymmetric due to stochastic particle motion, recirculation, and secondary flow structures that break symmetry. Centrifugal effects within the crucible also require full-domain resolution; using symmetry would artificially constrain particle dynamics and could misrepresent inclusion trajectories.

[1] AlTiB master alloy is added to the melt to form Al_3Ti particles on a pre-existing alumina bifilm.

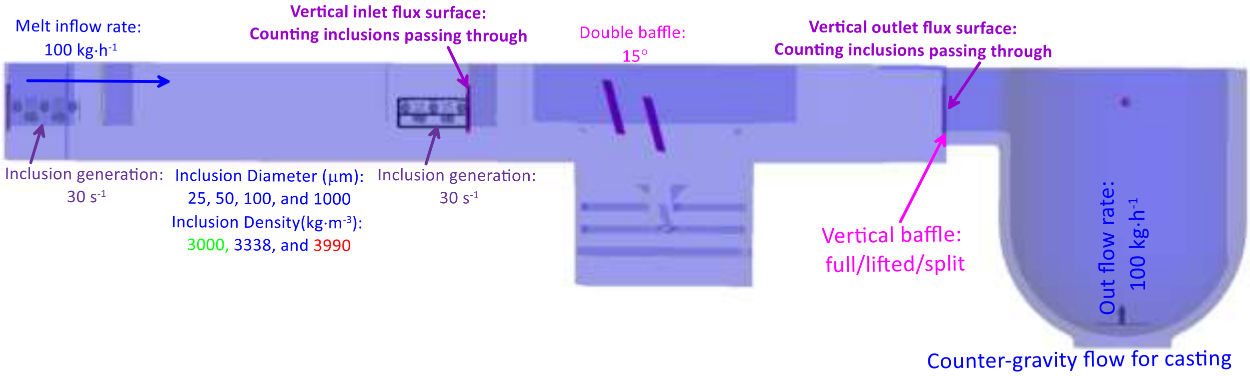

Fig. 1. The launder-crucible assembly with interchangeable baffle configurations at the interface. Due to proprietary design, only a limited side view is shown. Melt flows from left to right at 100 kg·h⁻¹. Inclusions of various sizes and densities form at the indicated position. The primary double baffles, set at 15° to vertical and inclined against flow, are in the sediment tank, while secondary baffles are at the launder-crucible interface, as in Figure 2.

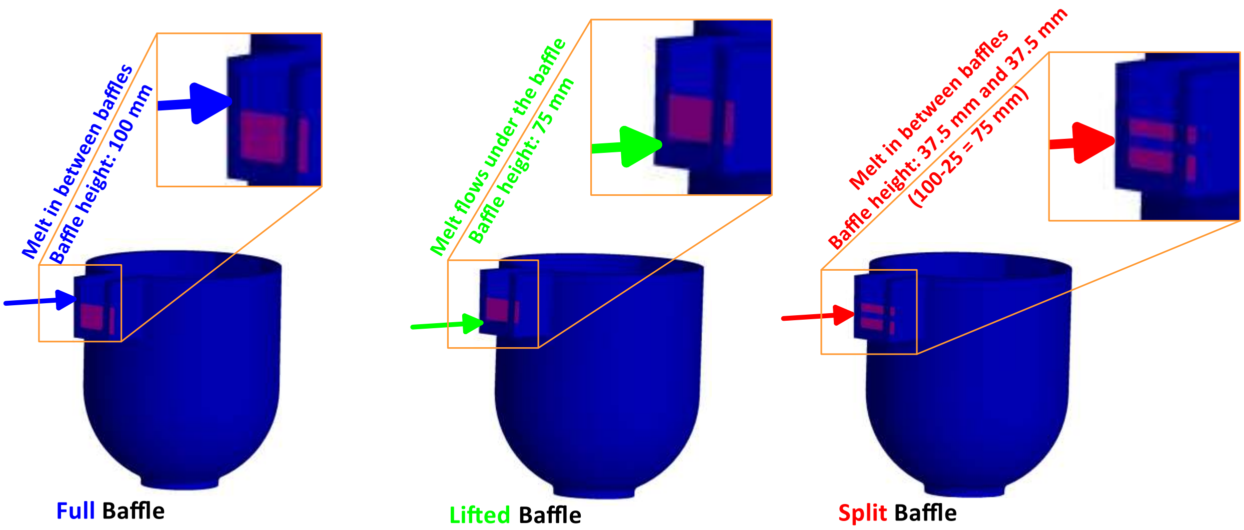

Fig. 2. Schematic illustration of the type baffles at the launder-crucible interface and their dimensions.

The influence of the baffle's setup on the melt flow behaviour and the sedimentation efficiency of inclusions is compared. Three secondary baffle configurations at the Launder-crucible interface were examined, Figure 2:

1. Full-baffle (Overflow-type): A full-height baffle that forces the melt to flow over the top edge.
2. Lifted-baffle (or Undershot-type) baffle: a raised baffle that allows melt to flow beneath through a defined clearance.
3. Split-baffle (or Slotted-): two partial-height baffles separated by a central slot.

Simulations were performed using a commercial computational fluid dynamics solver with Lagrangian particle tracking (Flow3D, Flow Science USA) at the Delta 2 high-performance computing facility at Cranfield University. Flow3D uses a finite-volume method for its simulations. The key parameters are summarised in Table 1. The results are then compared to determine which inclusions pass through the baffles or exit the system. Two particle counters were also added to the simulation setup: one at the launder-crucible interface and the other just before the melt enters the counter-gravity casting pump. Counting inclusions and comparing them will provide the sedimentation efficiency for each particle type, e.g., density and diameter. This way, it is possible to determine the baffle setup that results in cleaner melt exiting the system, following some of Campbell's [14] rules for good casting: a cleaner melt at a streamline flow to fill the mould cavity. That is, minimal entrained oxide bifilm or any other inclusion in the melt, and ensuring that none (optimal) form during the mould filling process, for better casting in structural high-end applications using secondary-sourced aluminium alloys. The Reynolds number, Table 1, indicates non-turbulent flow up to 4000 (a reasonable approximation accepted by the fluid dynamics research community) or 2300 for laminar flow. In this case, the value is approximately 160, which is significantly below the threshold required for stable streamline flow in the launder system at a flow rate of 100 $kg{\cdot}h^{-1}$ and a minimum cross-section of 100×100 mm^2; the fluid velocity should be approximately 1 $mm{\cdot}s^{-1}$ at this mass flow rate through the smallest cross-section of the launder. The Reynolds number, even at a velocity of 5 $mm{\cdot}s^{-1}$, would be around 800. This suggests that the flow could be increased to approximately 5000 $kg{\cdot}h^{-1}$ before turbulence occurs (a safe estimate).

Table 1. Summary of simulation parameters and operating conditions.

Description	Values
Alloy	aluminium-silicon alloy (A356 alloy). The simulation was carried out for liquid flow; therefore, there is no significant effect from minor chemical variations in the secondary-sourced alloy.
Liquidus	617.6 °C
Melt temperature	650 °C
Flow rate	0.028 $kg{\cdot}s^{-1}$ (~100 $kg{\cdot}h^{-1}$)
Inclusion density	3348 $kg{\cdot}m^{-3}$, and 3990 $kg{\cdot}m^{-3}$
Inclusion diameter	25 μm, 50 μm, 100 μm, and 1000 μm
Particle generation rate	30 s^{-1} (continuous/random)
External insulated wall temperature	200 °C (measured/fixed boundary condition)
Approximate dimensions of the launder crucible setup (proprietary design)	4×1×1 m^3, (crucible 1×1×1 m^3)
Mesh size	~ 6 mm (average)
High-performance computing wall time	~ 5 days per 3000 s simulation
Simulation time	22600 s (physical time)
Reynold number, $\frac{\rho V L}{\mu}$ (ρ-density, V-velocity, L-characteristic length of the cross section and is the side length of the square cross section, μ-dynamic viscosity of the fluid)	Around 160, at a melt flow rate of 100 $kg{\cdot}h^{-1}$ through the smallest section of the launder, 100×100 mm^2 square cross section.

Results

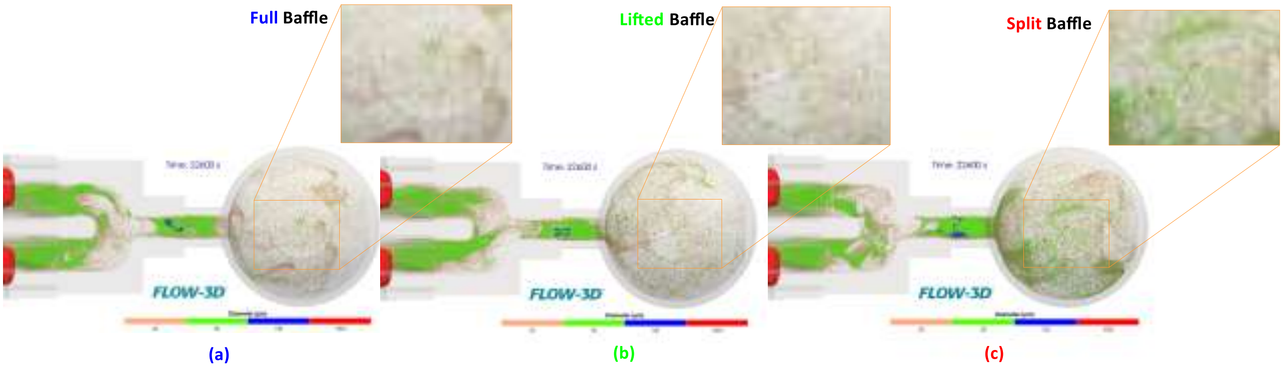

Fig. 3. Top view of inclusion distribution at 22600 s for (a) full-/ (b) lifted-/ (c) split- baffle, respectively. Due to the proprietary nature of the launder design, only a portion of the launder (hidden) view is presented. Only blue (25 µm) and brown-coloured (50 µm) inclusions can be seen in the crucible. The larger blue-coloured (100 µm) and red-coloured (1000 µm) inclusions have already sedimented in the sediment tank.

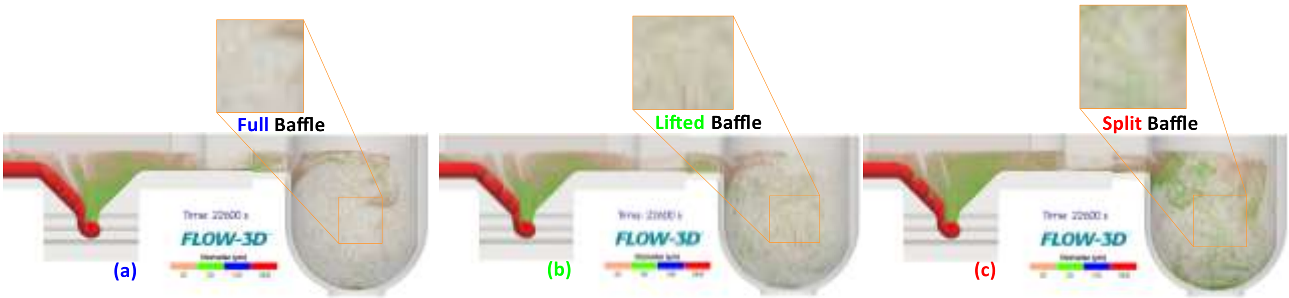

Fig. 4. Side views of inclusion distribution at 22600 s for the (a) full-/ (b) lifted-/ (c) split- baffle configurations, respectively. Due to the proprietary nature of the launder design, only a portion of the launder (hidden) view is presented. Only blue (25) and brown (50) coloured inclusions can be seen in the crucible. The larger blue-coloured (100) and red-coloured (1000) inclusions have already sedimented in the sediment tank.

A vast data set was collected from various simulations, and a detailed quantification study was considered 'not necessary'. However, a qualitative analysis of the time stage of the inclusions was deemed reasonably sufficient for comparison and was therefore evaluated and concluded accordingly. Although some quantification of the results is presented in Figure 5 to strengthen the conclusion. The simulation was run for approximately 22600 s (~6.3 h), which was assumed sufficient for the saturation duration in a practical casting trial. At the end of the 22600 s time, the positions of the inclusions are visualised and compared in Figures 3 (Top view) and Figure 4 (side view) of the crucible side of the simulation setup. The inclusions were enlarged for comparison. The red-coloured inclusions were 1000 µm in diameter, blue were 100 µm, green were 50 µm, and the 25 µm were brown in colour.

The full-baffle, Figure 3 (a) and Figure 4 (a), produces strong upstream deceleration and large recirculation zones. Denser and larger inclusions tend to stagnate upstream of the baffle, whereas smaller inclusions may pass into the crucible. The lifted-baffle configuration, Figure 3 (b) and 4 (b), promotes subsurface inflow and a less turbulent free surface. Inclusion trajectories follow smooth curved paths beneath the baffle, resulting in improved sedimentation and reduced re-entrainment. The split-baffle, Figure 3 (c) and Figure 4 (c), configuration produces a combined jet-recirculation flow. While flow uniformity is improved, a fraction of the minor inclusions bypasses the sedimentation region through the slot or the split section of the baffle. All baffle setups appear effective at controlling larger inclusions (> 50 µm). Although the lifted-/full- baffles seem to control even smaller inclusions, a small portion of 25 µm inclusions is still visible in the crucible. When comparing the effectiveness of these two baffle setups for sedimenting inclusions, the split baffle is less effective, as evidenced by the inclusions' positions later in the simulation and quantitative analysis, Figure 5. Quantifying the inclusion escape into the counter-gravity casting pump would be a future study, although it is not necessary to conclude that the lifted baffle was both technically and practically an effective solution for optimising the sedimentation of fine-scale inclusions as small as 25 µm in diameter. It is important to note that inclusion counting was performed only from 22000 s to 22900 s to compare the sedimentation efficiency of these baffles; it was not necessary to count from 0 s to 22900 s. This was considered a reasonably saturated time to minimise the computation time. A diverging plot does not necessarily mean that saturation was not achieved, as these plots were used for comparison only to show the total number of inclusions in each category at the end of the time period. The shape of the launder may have caused a pattern of inclusion passing through the flux surfaces. Based on the inclusion distribution in the crucible, this helps explain that the lifted baffle setup trapped finer inclusions more effectively than the split baffle.

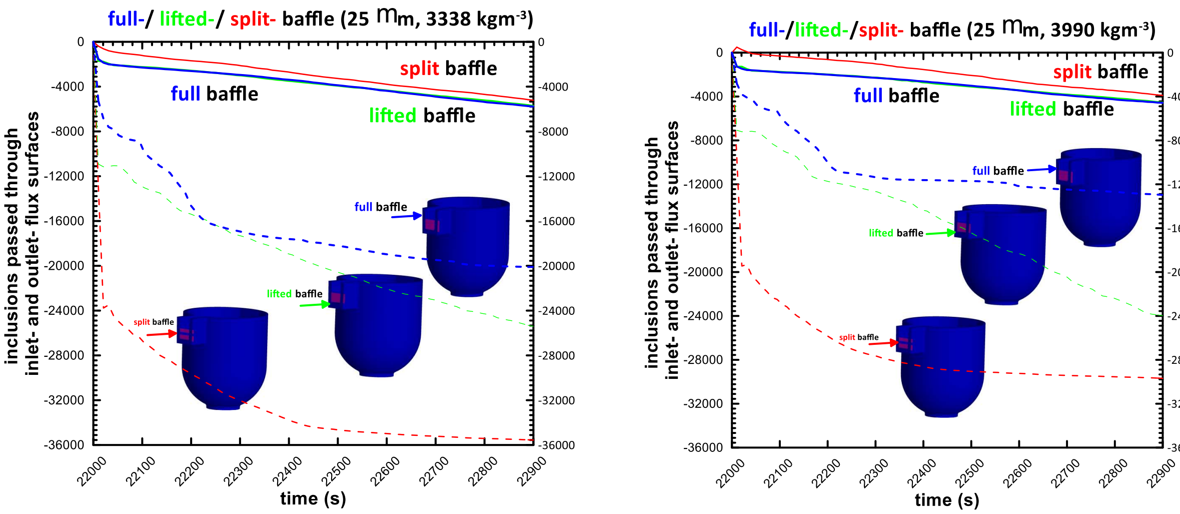

Fig. 5. The 25 µm diameter inclusions with densities of (left) 3338 kg·m^{-3} and (right) 3990 kg·m^{-3} passed through flux surfaces at (solid lines) the inlet and (dotted lines) outlet for the full-, lifted-, and split-baffle configurations. These inclusions moved through the inlet and outlet over time from 22000 s to 22900 s. The outlet flux surface captures more inclusions than the inlet because the suspended particles are in the launder. Note: the negative y-axis shows inclusions exiting the flux surface, and the background indicates the baffle setup at the launder interface for clarity.

Discussion

Comparative Sedimentation Performance

The three baffle configurations alter the local hydrodynamics at the launder-crucible interface in distinct ways. Full (overflow) baffles maximise upstream trapping but risk oxide generation, although they act as a baseline for comparison. Lifted (undershot) baffles provide a balanced combination of flow stability and sedimentation efficiency. Split (slotted) baffles offer moderate performance, with improved flow symmetry but reduced retention of 25 µm or 50 µm inclusions.

Centrifugal Flow Effects in the Crucible

The results indicated that inclusions of 25 µm and 50 µm mostly escaped, depending on the secondary baffle used. To explain the reasons and identify possible causes, it is vital to analyse the forces acting on these inclusions at a fundamental level. Each inclusion in the crucible experiences gravitational, buoyant, and centrifugal forces. Figure 6 shows the calculated minimum (brown line) and maximum (pink line) of the resultant vertical forces (the sum of the gravitational and buoyant forces, the horizontal lines). The plots (inclined lines) compare the centrifugal forces as a function of the inclusion velocity for various diameters and densities. The inclusion diameter (as marked, 1000 µm, 100 µm, 50 µm, 25 µm) has a significant effect on the forces, while the density (red/blue/green lines) has a minor effect. The lifted (undershot) baffle configuration induces a mild tangential velocity component within the crucible, generating centrifugal forces that guide inclusions toward the crucible wall. While smaller than gravity or buoyancy (Figure 6), these forces are directionally important and enhance the residence time of inclusions near low- and stagnation-velocity wall regions. The gravitational (/buoyancy) force/s on these inclusions are significantly larger than the centrifugal force that acts on inclusions of this study. They assist in moving inclusions towards stagnation (melt; inclusions still move due to gravity/sedimentation) velocity zones; hence, gravitational force could influence the sedimentation of these inclusions. Figure 6 compares the centrifugal forces on these inclusions as a function of diameter and velocity, along with the gravitational forces. At a certain threshold velocity, e.g., ~1 mm·s^{-1}, the 100 µm inclusions, the centrifugal force becomes comparable to gravitational and buoyant forces, and their influence is considered important. Because fine inclusions are difficult to sediment solely by gravity, the assistance of centrifugal forces brings them into the stagnation velocity zone; hence, gravity and prolonged residence time of these inclusions facilitate sedimentation. The critical velocity for which the centrifugal forces become comparable to the gravitational forces would be 2.5 mm·s^{-1} for 50 µm inclusions, as well as 5 mm·s^{-1} for the finer (25 µm) inclusions. A velocity of 5 mm·s^{-1} is not considered turbulent in casting conditions, which may not cause significant issues; however, it is only required in a portion of the crucible to generate the necessary centrifugal force to move the finer inclusions towards the stagnation zone, thereby optimising the sedimentation process. The effect of centrifugal force is therefore the reason the lifted baffle achieves higher efficiency in sedimenting inclusions. This brings the melt beneath the surface and circulates it to achieve a critical velocity that exceeds those of other baffle setups.

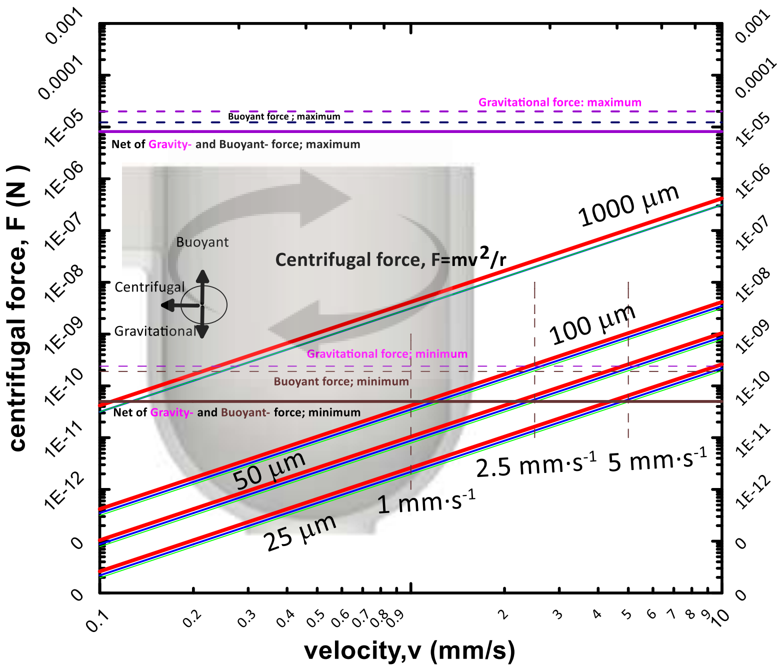

Fig. 6. Calculated centrifugal force, F, using the fundamental equation $F= mv^2/r$ (on a particle with mass, m, velocity,v, and the radius,r), acting on inclusions of different sizes and densities as a function of melt velocity (with random values within the domain of simulated inclusion velocity, 1, 2.5, and 5 mm·s^{-1}). The colour codes are red for high-density, blue for medium-density, and green for low-density inclusions. The crucible background shows forces acting on a particle and their directions.

Numerical and Computational Considerations

Long physical simulation times and large computational domains impose significant constraints even with a high-performance computer (HPC). The current setup represents a compromise among spatial resolution, simulation duration, and post-processing feasibility, as specified in Table 1. Although the mesh size (6000 μm or 6 mm) considered in this study may slightly misplace the inclusion positions, this ultimately alters the predicted positions of these inclusions. The inclusions had diameters of 25, 50 μm, 100 μm, and 1000 μm. These are 240, 120, 60, and 6 times smaller than the mesh size; while the mesh size was comparable for the 100 μm and 1000 μm inclusions, it was not for the 25 μm and 50 μm inclusions, which may significantly affect the position error for these inclusions. Balancing the mesh size comparable to the inclusion size is vital. In practice, it is a viable solution to find a Pareto front to determine a reasonable mesh size for computational and post-processing efficiency. Measurement and computational errors are inevitable; therefore, this Pareto front is a viable solution.

The Flow3D simulation employs a point-mass assumption for particles; therefore, inclusions are treated as non-interacting Lagrangian points, without inclusion-inclusion (particle-particle) collisions or agglomeration. Physical clustering is not possible in the present model. Any apparent grouping of inclusions observed in the visualisations is a visual illusion caused by the projection of inclusions travelling along similar flow paths and residence-time patterns. In addition, the particles were intentionally enlarged in the post-processing visualisation for clarity, which may further enhance the perception of clustering. This effect is purely graphical and does not represent physical agglomeration.

Practical Implications

The simulation assumes isothermal conditions (the measured external temperature of 200 °C) **only at the external boundary**, because the launder is insulated and operates in a controlled casting environment with heating elements surrounding it (top surface and some near the sediment tank). The low Reynolds number (laminar flow) minimises viscous heating. In industrial launders, thermal gradients are usually small relative to hydrodynamic effects. Although thermal losses near the walls can slightly increase viscosity and affect local flow, their impact on inclusion distribution is secondary to factors such as residence time and gravity-driven sedimentation. From an industrial perspective, the lifted (undershot-type) baffle is the most feasible option. It minimises surface disturbance, limits oxide formation, and provides effective inclusion filtration, while remaining compatible with continuous counter-gravity casting systems. The split baffle may also pose a practical challenge during melt delivery, whereas the lifted baffle may be easier to place in the launder system and may not significantly cause oxide reformation issues. Baffle optimisation through different geometries (split/lifted) and positioning, control inclusion path lines and accumulation zones. The sedimentation performance trend was as follows:

Full baffle ~ Lifted baffle > Split baffle, for smaller and lighter inclusions

Split baffle still seems sufficient for denser (3990 kg·m^{-3} >) and larger (100 μm >) inclusions

In practical situations, adjustable baffle height and inclination can provide tunable melt-cleaning performance that adapts to varying inclusion types and melt flow rates. Inclusion/particle trapping at the low flow rate of 0.028 kg·s^{-1} (~100 kg·h^{-1}) is significantly better for inclusions of various sizes and densities within the launder. The slower flow gives inclusions more residence time to settle or float. At a higher flow rate (e.g., from a previous study, 180 kg·h^{-1}), smaller inclusions remain suspended longer and are more likely to escape, while larger, denser inclusions still settle but less uniformly. On the other hand, this low flow rate may be suitable for aerospace casting, whereas automotive casting requires a much higher flow rate to optimise production. In automotive production, the inclusion size tolerance is less stringent than in aerospace. The presence of primary/secondary baffles, or their angles, significantly enhances inclusion sedimentation. As demonstrated in another study [9], inclined baffles at 15° or 30° improve the filtration of small (~25 µm) or low-density inclusions, whereas larger (>50 µm) and high-density inclusions settle completely within the launder. This study reveals that further refinement of these fine inclusions can be achieved by adding a secondary baffle at the launder-crucible interface, with an appropriate opening for melt flow. Therefore, a correlation between flow rate, launder/crucible/baffle designs and the particle properties should be identified. A unified solution may be impractical, or further research is required. However, suitable primary, secondary, and tertiary baffle designs can increase inclusion residence time to achieve effective sedimentation and provide a cleaner and smoother melt supply for casting structural components with high tolerances for physical and mechanical properties.

Conclusions

- Baffle design at the launder-crucible interface strongly influences inclusion transport and sedimentation efficiency.
- The undershot baffle provides the best balance between melt stability and inclusion filtration.
- Mild centrifugal flow within the crucible enhances final-stage sedimentation in the crucible.
- Integrated optimisation of the launder and crucible setup with suitable baffles enables cleaner, more automated melt delivery for structural aluminium castings.

Acknowledgements

The authors gratefully acknowledge the valuable and continuous support for the UltraCleanCAST DLMM project from Prof. John Campbell. The financial support from UK Research and Innovation through the UltraCleanCAST DLMM project is also gratefully acknowledged. Appreciation is extended to the Delta2 High Performance Computer team at Cranfield University and to Flow Science for providing a discounted academic research licence for Flow 3D products. Their collaboration and resources have been crucial to the progress of the UltracleanCAST DLMM project.

References

[1] Campbell J. The consolidation of metals: the origin of bifilms. Journal of Materials Science 2016;51. https://doi.org/10.1007/s10853-015-9399-9.

[2] Dispinar D, Campbell J. Use of bifilm index as an assessment of liquid metal quality. International Journal of Cast Metals Research 2006; 19. https://doi.org/10.1179/136404606225023300.

[3] El-Sayed MA. The behaviour of bifilm defects in cast Al-7Si-Mg alloy. PLoS One 2016;11. https://doi.org/10.1371/journal.pone.0160633.

[4] Zhang L, Taniguchi S, Cai K. Fluid flow and inclusion removal in continuous casting tundish. Metallurgica and Materials Transactions B 2000;31:253–66. https://doi.org/10.1007/s11663-000-0044-9.

[5] Fang Q, Zhang H, Luo R, Liu C, Wang Y, Ni H. Optimisation of flow, heat transfer and inclusion removal behaviours in an odd multistrand bloom casting tundish. Journal of Materials Research and Technology 2020;9. https://doi.org/10.1016/j.jmrt.2019.10.064.

[6] He Z, Zhou K, Liu S, Xiong W, Li B. Numerical modelling of the fluid flow in continuous casting tundish with different control devices. Abstract and Applied Analysis 2013;2013. https://doi.org/10.1155/2013/984894.

[7] Liu G, Ren Y, Ma W, Morita K, Lei Y, Zhan S, et al. Recent advances and future trends of aluminium alloy melt purification: A review. Journal of Materials Research and Technology 2024;28:4647–62. https://doi.org/10.1016/J.JMRT.2024.01.024.

[8] TU Delf Open Courseware. Sedimentation; WATER TREATMENT. n.d.

[9] T Sivarupan et al. Baffle-Based Sedimentation Strategies for Inclusions in Launders of Aerospace Aluminium Casting: A Sustainable Approach. 2026 TMS Annual Meeting & Exhibition, 2026.

[10] Griffiths WD, Beshay Y, Parker DJ, Fan X, Hausard M. The application of positron emission particle tracking (PEPT) to study the movement of inclusions in shape castings. Shape Casting: 3rd International Symposium 2009.

[11] Burnard DJ. Positron Emission Particle tracking of inclusions in cast liquid metals. 2015.

[12] Salonitis K, Jolly MR, Zeng B, Mehrabi H. Improvements in energy consumption and environmental impact by novel single-shot melting process for casting. Journal of Cleaner Production 2016;137:1532–42. https://doi.org/https://doi.org/10.1016/j.jclepro.2016.06.165.

[13] Sivarupan T, Palanivel AMVJ, Georgarakis K, Forde J, Rawding J, Shaw B, et al. Sedimentation of Inclusions in Melts of Aerospace Structural Aluminium Alloy Castings: A Sustainable Approach. In: Edwards L, editor. Light Metals 2025, Cham: Springer Nature Switzerland; 2025, p. 1172–9.

[14] Campbell J. Complete Casting Handbook: Metal Casting Processes, Metallurgy, Techniques and Design: Second Edition. 2015. https://doi.org/10.1016/C2014-0-01548-1.